

# Synthesis and Dynamic Behavior of the Dimeric, Monocyclic Barium Bis[bis(isopropyldimethylsilyl)phosphanide] – Molecular Structures of $\text{P}(\text{SiMe}_2\text{Ph})_3$ , of Monomeric $(\text{thf})_4\text{Ba}[\text{P}(\text{SiMe}_2i\text{Pr})_2]_2$ and of the Dimer $\{(\text{thf})_2\text{Ba}[\text{P}(\text{SiMe}_2i\text{Pr})_2]_2\}_2$

Matthias Westerhausen\*, Gerhard Lang, and Wolfgang Schwarz

Institut für Anorganische Chemie der Universität Stuttgart,  
Pfaffenwaldring 55, D-70550 Stuttgart, Germany  
Telefax: (internat.) +49(0)711/685-4241  
E-mail: westerhausen@anorg55.chemie.uni-stuttgart.de

Received April 10, 1996

**Key Words:** Phosphanes / Bis(silyl)phosphanes / Tris(silyl)phosphanes / Phosphanides / Barium bis(phosphanide)

Barium bis[bis(trimethylsilyl)amide] metalates bis(isopropyldimethylsilyl)phosphane (**1**) to yield nearly quantitatively the corresponding barium bis[bis(isopropyldimethylsilyl)phosphanide] (**3**). This compound shows a temperature-dependent monomer-dimer equilibrium in toluene solution. Both the isomers were characterized by X-ray crystal structure analyses. The monomeric derivatives precipitate as a tetra-

kis(tetrahydrofuran) complex with a P–Ba–P bond angle of  $139.9^\circ$ . The barium atoms of the monocyclic, centrosymmetric dimer are pentacoordinated by two tetrahydrofuran molecules, one terminal and two bridging phosphanide ligands. The endo- and exocyclic Ba–P distances with values of 332 and 316 pm, respectively, lie within the characteristic range.

The solvent-free dimeric alkaline earth metal bis[bis(trimethylsilyl)amides] crystallize as monocyclic molecules of the type  $\text{R}_2\text{N}-\text{M}(\mu\text{-NR}_2)_2\text{M}-\text{NR}_2$ <sup>[1]</sup>. In toluene the derivatives of calcium, strontium, and barium remain dimeric, whereas for the magnesium compound a monomer-dimer equilibrium<sup>[2]</sup> is observed.

In contrast to these amides, the homologous phosphanides show a unique behavior. Dimeric strontium bis[bis(trimethylsilyl)phosphanide] dissolved in toluene is monomeric as a tetrakis(tetrahydrofuran) complex at low temperatures, at room temperature a dimeric species of the type  $\text{R}_2\text{P}-\text{Sr}(\mu\text{-PR}_2)_3\text{Sr}(\text{thf})_3$  predominates<sup>[3]</sup>. Two years later Rabe and coworkers<sup>[4]</sup> isolated an isotopic samarium bis[bis(trimethylsilyl)phosphanide], which demonstrates that the alkaline earth metal bis(phosphanides) resemble more the structures of the lanthanoids than of the main group metals such as lithium<sup>[5]</sup> or zinc<sup>[6]</sup>. A structure with a similar framework was isolated for tris(1,2-dimethoxyethane)di-barium tetrakis(2,2,5,5-tetramethyl-2,5-disila-1-phosphacyclopentane)<sup>[7]</sup>. These phosphanides of strontium and barium show a dynamic behavior in toluene; the dimerization with loss of coordinated solvent molecules such as tetrahydrofuran or dimethoxyethane increases with rising temperature.

Moreover, ab-initio SCF calculations on the dimeric alkaline earth metal bis(phosphanides)  $\{\text{M}(\text{PH}_2)_2\}_2$ <sup>[8]</sup> revealed an energetic minimum for the  $C_1$  symmetric isomer of the type  $\text{H}_2\text{P}-\text{M}(\mu\text{-PH}_2)_3\text{M}$  for the metals calcium and strontium (Table 1). For the barium derivative even the quadruple-bridged  $D_{4h}$  symmetric molecule  $\text{Ba}(\mu\text{-PH}_2)_4\text{Ba}$  is favored. However, the influence of solvent molecules was

not taken into account. In this paper we describe a sterically enforced monocyclic dimer of  $\text{Ba}[\text{P}(\text{SiMe}_2i\text{Pr})_2]_2$  and compare the structural data with those of the monomeric derivative and the homoleptic tris(dimethylphenylsilyl)phosphane.

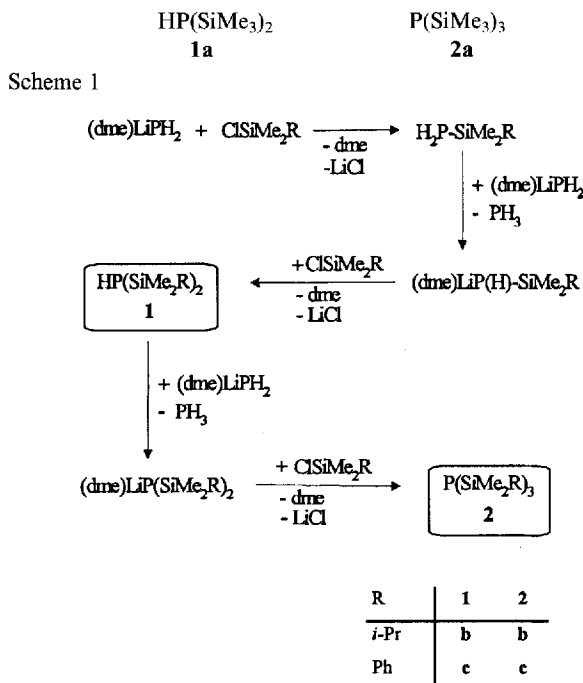
Table 1. Ab-initio SCF calculations of relative energies [ $\text{kJ mol}^{-1}$ ] for the monocyclic, bicyclic, and tricyclic dimers  $[\text{M}(\text{PH}_2)_2]_2$  of the types  $\text{X}-\text{M}(\mu\text{-X})_2\text{M}-\text{X}$  ( $C_{2h}$  symmetry),  $\text{X}-\text{M}(\mu\text{-X})_3\text{M}$  ( $C_1$  symmetry), and  $\text{M}(\mu\text{-X})_4\text{M}$  ( $D_{4h}$  symmetry), respectively

| M                     | Mg    | Ca   | Sr   | Ba   |
|-----------------------|-------|------|------|------|
| $C_{2h}$ (monocyclic) | 0     | 51.6 | 41.3 | 60.0 |
| $C_1$ (bicyclic)      | 27.9  | 0    | 0    | 8.0  |
| $D_{4h}$ (tricyclic)  | 212.3 | 44.2 | 17.9 | 0    |

## Preparation

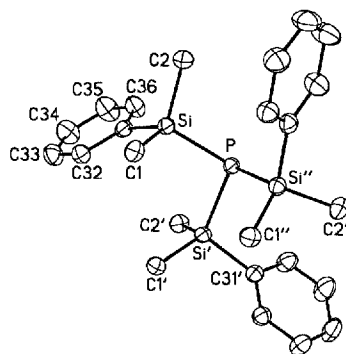
For the synthesis of substituted bis(silyl)phosphanes  $\text{HP}(\text{SiMe}_2\text{R})_2$  two routes were applied earlier. Bis(trimethylsilyl)phosphane was obtained by protolysis of tris(trimethylsilyl)phosphane<sup>[9]</sup>, isolated from the reaction of  $\text{Na}_3\text{P}/\text{K}_3\text{P}$  with chlorotrimethylsilane in ether such as 1,2-dimethoxyethane<sup>[10]</sup>. The metathesis reaction of  $(\text{dme})\text{LiPH}_2$ <sup>[11]</sup> with chlorotriorganysilane yielded a mixture of the phosphanes  $\text{H}_{3-n}\text{P}(\text{SiMe}_2\text{R})_n$  [ $n = 2$ : **1**,  $n = 3$ : **2**;  $\text{R} = \text{Me}$  (**a**),  $i\text{Pr}$  (**b**),  $\text{Ph}$  (**c**)] according to the reaction sequence shown in Scheme 1<sup>[7]</sup>. The mixture has to be separated by distillation. The yields strongly depend on the steric demand of the triorganysilyl substituent, but due to a significant difference in the boiling points pure bis(dimethylorganylsilyl)-

phosphanes **1** were isolated. To achieve higher yields and a higher purity of the tris(triorganylsilyl)phosphanes **2** the synthesis in analogy to the preparation of tris(trimethylsilyl)phosphane using the sodium potassium alloy, phosphorus and an excess of chlorotriorganylsilane is highly recommended<sup>[12]</sup>.



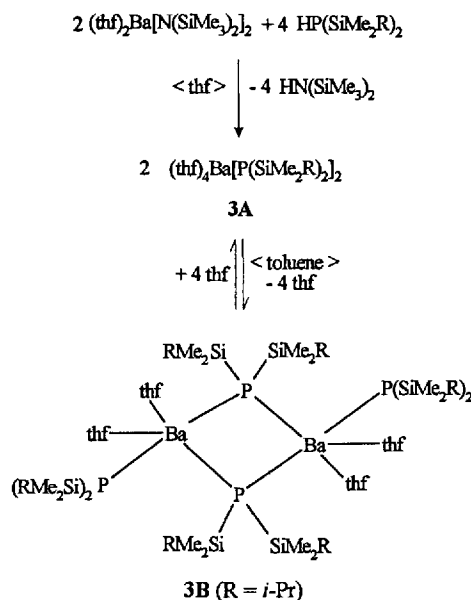
Tris(dimethylphenylsilyl)phosphane (**2c**) is a sublimable solid<sup>[12]</sup>. The structural parameters of this sterically not overcrowded phosphane can serve as a reference due to the lack of steric strain. The molecular structure of phosphane **2c** and the numbering scheme are represented in Figure 1. The molecule shows crystallographically enforced  $C_3$  symmetry. The atoms generated by the  $C_3$  rotational axis are marked with primes. The phosphorus atom is surrounded pyramidically by Si–P–Si bond angles of  $104^\circ$ . The P–Si distances with values of 225.7 pm lie in the range characteristic of triorganylsilyl-substituted phosphanes<sup>[7,13]</sup>.

Figure 1. Molecular structure of **2c**. Thermal ellipsoids are drawn at the 50% probability level. The hydrogen atoms are omitted for clarity. Symmetry-related atoms are marked with primes. Selected bond lengths [pm]: P–Si 225.7(1), Si–C1 187.6(3), Si–C2 186.7(3), Si–C31 188.2(2); selected bond angles [ $^\circ$ ]: Si–P–Si' 103.98(3), P–Si–C1 116.30(8), P–Si–C2 108.07(9), P–Si–C31 105.55(8).



The metalation of bis(isopropyldimethylsilyl)phosphane (**1b**) with barium bis[bis(trimethylsilyl)amide]<sup>[2]</sup> in tetrahydrofuran yielded nearly quantitatively the corresponding barium bis[bis(isopropyldimethylsilyl)phosphanide] (**3**) according to Scheme 2. Recrystallization from tetrahydrofuran allowed the isolation of a tetrakis(tetrahydrofuran) adduct **3A**, whereas the precipitation from a toluene solution led to the crystallization of the dimeric, monocyclic molecule **3B**. Both these compounds are moisture- and air-sensitive.

Scheme 2



## NMR Spectroscopy

The phosphanes **1** and **2** differing only in one of the organyl groups at the silicon atom exhibit very similar NMR parameters as listed in Table 2. The  $^1J(\text{P-H})$  coupling constants of **1** lie around 190 Hz, the chemical shift of the PH proton varies between  $\delta = 0.5$  and 1. The steric demand of the isopropyl substituent leads to a remarkable high-field shift in the  $^{31}\text{P}\{^1\text{H}\}$ -NMR spectrum and low-field shift for the  $^{29}\text{Si}$  nucleus. The  $^1J(\text{P-Si})$  value varies between 25 and 30 Hz. A comparison of the phosphanes **1** and **2** clearly demonstrates that the steric demand of the isopropyl substituent exceeds the electronic influence of the phenyl group.

The  $^{31}\text{P}\{^1\text{H}\}$ -NMR spectra of the barium complex **3** show a strong temperature dependence (Figure 2). At  $-60^\circ\text{C}$  a sharp singlet at  $\delta = -274.3$  for the monomeric derivative **3A** and a very broad signal at  $\delta = -240$  for the dimer **3B** are observed. With rising temperature the high-field shifted signal of the monomer diminishes. At the same time the broad signal of **3B** is shifted downfield to  $\delta = -226$  and becomes narrower. The exchange of the phosphanide ligands between the terminal and the bridging position even at 210 K is so fast on the NMR time scale that all the spectra were recorded above the coalescence temperature. Scheme 3 displays the equilibrium without rep-

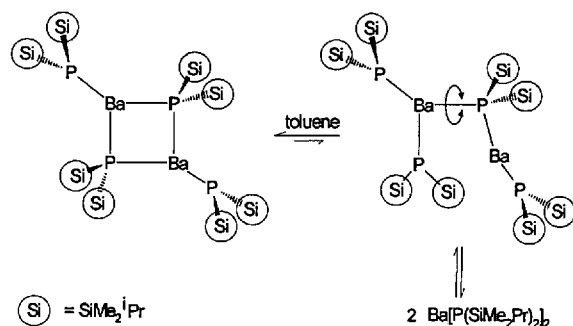
Table 2. NMR data of the phosphanes  $\text{HP}(\text{SiMe}_2\text{R})_2$  ( $\text{R} = \text{Me}$  **1a**<sup>[9,14]</sup>, *i*Pr **1b**, and Ph **1c**) and  $\text{P}(\text{SiMe}_2\text{R})_3$  ( $\text{R} = \text{Me}$  **2a**<sup>[10]</sup>, *i*Pr **2b**, and Ph **2c**<sup>[12]</sup>),  $[\text{D}_6]\text{benzene}$ , 30 °C

| Compound                                 | <b>1a</b> | <b>1b</b> | <b>1c</b> | <b>2a</b> | <b>2b</b> | <b>2c</b> |
|------------------------------------------|-----------|-----------|-----------|-----------|-----------|-----------|
| <sup>1</sup> H:                          |           |           |           |           |           |           |
| δ(P-H)                                   | 0.63      | 0.51      | 0.95      |           |           |           |
| <sup>1</sup> J(P-H)                      | 187.0     | 190.9     | 190.3     |           |           |           |
| δ(Me)                                    | 0.21      | 0.19      | 0.29      | 0.24      | 0.24      | 0.32      |
| <sup>3</sup> J(P-H)                      | 4.4       | 3.7       | 4.2       | 4.5       | 3.5       | 3.9       |
| δ(R)                                     | 0.21      | 1.01[a]   | 6.99-     | 0.24      | 1.03[a]   | 6.93-     |
|                                          |           | 0.99[b]   | 7.53      |           | 1.02[b]   | 7.65      |
| <sup>13</sup> C{ <sup>1</sup> H}: δ(Me)  | 3.39      | -0.50     | 1.46      | 4.39      | -0.14     | 2.41      |
| <sup>2</sup> J(P-C)                      | 10.7      | 7.9       | 11.1      | 11.3      | 7.1       | 10.6      |
| δ(R)                                     | 3.39      | 16.90[a]  | 139.60    | 4.39      | 16.75[a]  | 140.19    |
| <sup>2</sup> J(P-C)                      | 10.7      | 12.3      | 8.9       | 11.3      | 14.7      | 11.5      |
| δ(R)                                     |           | 17.90[b]  | 133.90    |           | 18.01[b]  | 134.41    |
| <sup>3</sup> J(P-C)                      |           | 3.5       | 2.8       |           | 4.8       | 3.4       |
| δ(R)                                     |           |           | 128.19    |           |           | 127.99    |
| <sup>4</sup> J(P-C)                      |           |           | <0.5      |           |           | <0.5      |
| δ(R)                                     |           |           | 129.42    |           |           | 129.25    |
| <sup>5</sup> J(P-C)                      |           |           | 0.5       |           |           | 0.6       |
| <sup>29</sup> Si{ <sup>1</sup> H}: δ(Si) | 3.22      | 10.20     | -1.38     | 0.40      | 10.01     | -1.49     |
| <sup>1</sup> J(P-Si)                     | 25.1      | 29.4      | 26.0      | 27.1      | 29.9      | 26.2      |
| <sup>31</sup> P{ <sup>1</sup> H}: δ(P)   | -235.7    | -258.5    | -237.4    | -251.4    | -274.5    | -247.3    |

[a] CH moiety of the isopropyl group. – [b] Methyl group of the isopropyl substituent.

resentation of the solvating tetrahydrofuran molecules. A very similar dynamic behavior exists for the dimeric solvent-free alkaline earth metal bis[bis(trimethylsilyl)amides] in toluene and benzene solution<sup>[2]</sup>. Here the terminal and bridging ligands are indistinguishable in the case of the barium derivative. However, a similar exchange process was found for the calcium and strontium bis[bis(trimethylsilyl)amides].

Scheme 3



The  $^{29}\text{Si}\{^1\text{H}\}$ -NMR spectrum recorded at room temperature shows a doublet at  $\delta = 9.03$  with a  $^1J(\text{P-Si})$  coupling constant of 39.1 Hz for dimeric **3B** (Figure 3). The exchange of the phosphanide ligands between the terminal and bridging site is fast on the NMR time scale. With decreasing temperatures the second doublet assigned to the monomeric isomer **3A** at  $\delta = 9.43$  with a  $^1J(\text{P-Si})$  value of 22.6 Hz arises.

Figure 2. Dynamic  $^{31}\text{P}\{^1\text{H}\}$ -NMR experiments of a  $[\text{D}_8]\text{toluene}$  solution of **3** (81.015 MHz, see text). The high-field signal belongs to the monomeric compound **3A**, the broad low-field resonance to the dimer **3B**

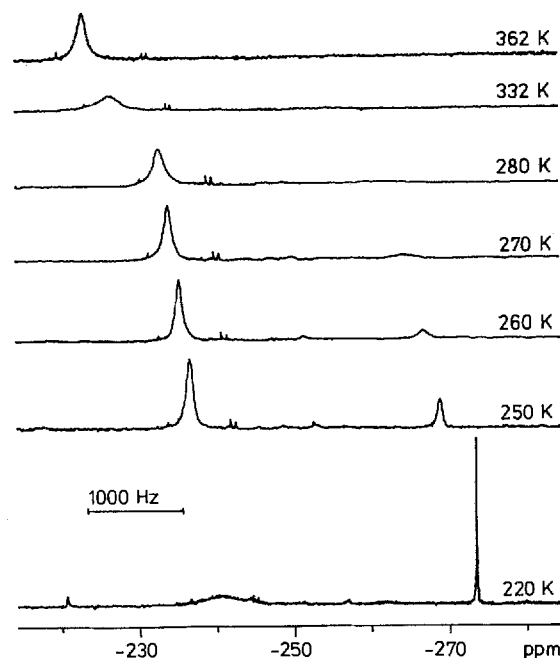
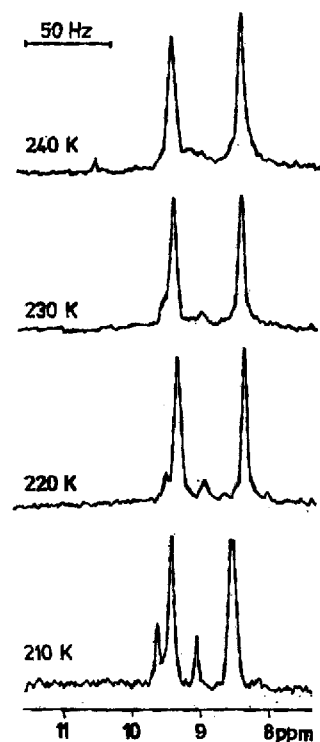


Figure 3.  $^{29}\text{Si}\{^1\text{H}\}$ -NMR measurements of **3** at variable temperatures in  $[\text{D}_8]\text{toluene}$  solution (39.761 MHz, see text)

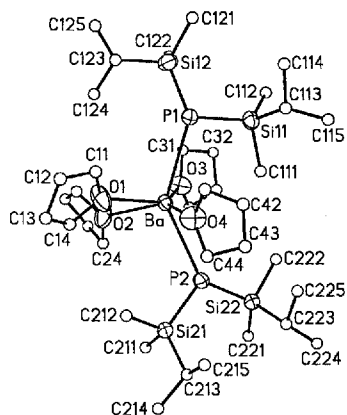


## Molecular Structures

At low temperature in the presence of an excess of tetrahydrofuran monomeric **3A** forms colorless cubic crystals.

The molecular structure and the numbering scheme are presented in Figure 4. The two phosphanide ligands are distinguished by the first number  $n$  following the element symbol. The barium atom is hexacoordinated by the two phosphorus and four oxygen atoms. The coordination polyhedron is best described as a pentagonal bipyramid with the phosphanide substituents in an axial position and the tetrahydrofuran molecules in the equatorial plane, where one of the sites is vacant due to the steric demand of the isopropyl groups at the silicon atoms Si(n2). The expected O–Ba–O bond angles within a pentagonal plane are  $72^\circ$ . In this molecule the O–Ba–O angles between neighboring tetrahydrofuran ligands vary between  $70$  and  $74^\circ$ , whereas the gap O3–Ba–O4 displays an angle of  $148^\circ$ . Furthermore, the P1–Ba–P2 moiety with a value of  $140^\circ$  is bent towards the vacant site located in the pentagonal-bipyramidal plane.

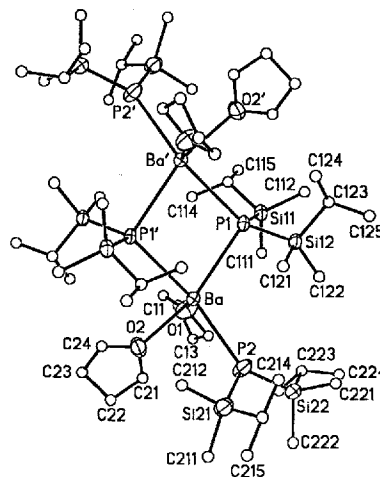
Figure 4. Molecular structure of monomeric **3A**. The thermal ellipsoids represent a 50% probability level. The hydrogen atoms are neglected for clarity. The carbon atoms are drawn with arbitrary radii. Selected bond lengths [pm]: Ba–P1 320.0(1), Ba–P2 318.4(1), Ba–O1 274.7(4), Ba–O2 272.4(4), Ba–O3 277.2(4), Ba–O4 275.7(4), P1–Si11 219.3(2), P1–Si12 218.4(2), P2–Si21 220.9(3), P2–Si22 219.6(3); selected bond angles [ $^\circ$ ]: P1–Ba–P2 139.93(3), Ba–P1–Si11 100.45(6), Ba–P1–Si12 132.38(7), Si11–P1–Si12 108.96(9), Ba–P2–Si21 113.64(7), Ba–P2–Si22 140.62(8), Si21–P2–Si22 105.70(10)



The P–Si distances are strongly shortened compared with those of the phosphane **2c** or tris(trimethylsilyl)phosphane (**2a**)<sup>[13]</sup>. Even though the phosphorus atoms display a nearly planar geometry, no backbonding from the phosphorus to the barium atom can be assumed due to the lack of a shortening of the Ba–P distances in comparison with similar compounds. The coordination number of the metal center and the pnictogen atoms dominate the bond lengths in these mainly ionic compounds.

Crystallization of **3** by cooling a saturated hot toluene solution to room temperature yielded the dimeric complex **3B**. Figure 5 shows the molecular structure and the numbering scheme. In contrast to the dimeric barium bis(phosphanides) investigated earlier<sup>[7]</sup>, **3B** crystallizes as a centrosymmetric monocyclic dimer with two bridging and two terminal phosphanide ligands. The barium atom is pentacoordinated by two ether oxygen and three phosphorus atoms. Due to the crystallographic inversion center the molecule

Figure 5. Molecular structure of the dimer **3B**. The ellipsoids represent a probability of 50%. The hydrogen atoms are omitted for clarity, the carbon atoms are drawn with arbitrary radii. Symmetry-related atoms are marked with primes. Selected bond lengths [pm]: Ba–P1 332.5(2), Ba–P1' 331.3(2), Ba–P2 316.1(2), Ba–O1 267.3(4), Ba–O2 273.2(4), P1–Si11 222.8(2), P1–Si12 222.6(2), P2–Si21 221.3(3), P2–Si22 220.0(2); selected bond angles [ $^\circ$ ]: P1–Ba–P1' 79.81(4), P1–Ba–P2 110.36(5), P2–Ba–P1' 156.80(4), Ba–P1–Ba' 100.19(4), Si11–P1–Si12 102.69(7), Ba–P1–Si11 110.89(6), Ba–P1–Si12 102.01(6), Ba'–P1–Si11 105.57(6), Ba'–P1–Si12 134.58(7), Si21–P2–Si22 104.83(9), Ba–P2–Si21 113.66(8), Ba–P2–Si22 141.19(8)



exists as a *trans* isomer. The endocyclic P–Ba–P angle amounts to  $79.8^\circ$ .

The terminal Ba–P2 distance of 316 pm lies in the narrow range of Ba–P bond lengths to tricoordinated phosphorus atoms<sup>[15,16]</sup>. The endocyclic Ba–P distances of 332 pm are only slightly longer than those in  $(\text{Me}_3\text{Si})_2\text{N}-\text{Ba}(\text{dme})[\mu-\text{P}(\text{SiMe}_3)_2\text{Ba}(\text{dme})\text{N}(\text{SiMe}_3)_2]$  (329 pm<sup>[16]</sup>). The terminal phosphorus atom P2 is nearly planar-coordinated. However, one of the silicon atoms (Si21/Si2A) is disordered. The coordination sphere of the terminal phosphanide ligand with Ba–P–Si angles of  $141$  and  $113^\circ$  is very unsymmetrical due to steric repulsion between these substituents and the solvated tetrahydrofuran molecules.

## Conclusion

The barium bis[bis(trialkylsilyl)phosphanides] show a monomer-dimer equilibrium in toluene solution with a predominance of the dimer at room temperature. Whereas the bicyclic species  $\text{R}-\text{Ba}(\mu-\text{R})_3\text{Ba}$  with small trialkylsilyl groups is favored, the monocyclic isomer of the type  $\text{R}-\text{Ba}(\mu-\text{R})_2\text{Ba}-\text{R}$  exists with the sterically demanding isopropyl dimethylsilyl substituent. A second dynamic process leads to an exchange of the bridging and terminal phosphanide ligands which cannot be frozen in the case of the monocyclic derivative even on cooling to 210 K.

We thank the *Deutsche Forschungsgemeinschaft*, Bonn, and the *Fonds der Chemischen Industrie*, Frankfurt a. M., for their generous financial support.

## Experimental

All experiments and manipulations were carried out under argon purified by passage through BTS catalyst<sup>[17]</sup> and  $\text{P}_4\text{O}_{10}$ . Reactions

were performed by using standard Schlenk techniques and dried, thoroughly deoxygenated solvents. The starting materials (dme)-LiPH<sub>2</sub><sup>[11]</sup> and Ba[N(SiMe<sub>3</sub>)<sub>2</sub>]<sub>2</sub><sup>[2]</sup> were prepared by literature procedures. — NMR: Bruker AM200 and AC250. All <sup>31</sup>P{<sup>1</sup>H}-NMR spectra are referenced to an external standard of 85% phosphoric acid. — IR: Perkin-Elmer 883 (intensities: very strong vs, strong s, medium strong m, weak w, broad br, shoulder sh). — To reduce the formation of metal carbides during elemental analyses V<sub>2</sub>O<sub>5</sub> was added. — Melting points: measured in capillaries sealed under argon.

**Bis(isopropyl)dimethylsilyl]phosphane (1b):** 28.8 ml of chloroisopropylidimethylsilane (25.0 g, 183 mmol) was dropped to a solution of 23.5 g of (1,2-dimethoxyethane)lithium phosphanide (181 mmol) in 150 ml of tetrahydrofuran at 0°C. After stirring of the mixture overnight at room temp., the precipitated lithium chloride was removed by filtration. After removal of the solvent, a vacuum distillation yielded 17.0 g of colorless **1b** (39.1 mmol, 43%) and 1.2 g of colorless **2b** (3.6 mmol, 6%). **1b**: B.p. 54–56°C/0.1 mbar. — NMR: See Table 2. — IR:  $\tilde{\nu}$  = 2954 vs, 2891 m, 2863 s, 2724 w, 2281 w, 1462 m, 1408 w, 1382 w, 1364 w, 1248 s, 1068 w, 998 m, 918 w, 881 s, 836 vs, 799 vs, 778 s, 686 m, 590 m, 459 m. — MS (70 eV), *m/z* (%): 234 (24) [M<sup>+</sup>], 219 (4) [M<sup>+</sup> – Me], 192 (30) [M<sup>+</sup> – C<sub>3</sub>H<sub>7</sub>], 149 (52), 101 (31), 73 (100) [SiMe<sub>3</sub><sup>+</sup>]. — PSi<sub>2</sub>C<sub>10</sub>H<sub>27</sub> (234.5): calcd. C 51.22, H 11.61; found C 51.09, H 11.60. — **2b**: B.p. 102°C/0.1 mbar. NMR: See Table 2. — C<sub>15</sub>H<sub>39</sub>PSi<sub>3</sub> (334.7): calcd. C 53.82, H 11.75; found C 53.69, H 11.73.

**Bis(dimethylphenylsilyl)phosphane (1c):** A solution of 18.3 g of (1,2-dimethoxyethane)lithium phosphanide (141 mmol) in 150 ml of tetrahydrofuran was cooled to 0°C. 24.6 ml of chlorodimethylphenylsilane (25.0 g; 146 mmol) was added dropwise. The solution turned reddish brown. After stirring overnight at room temp., lithium chloride was removed by filtration and tetrahydrofuran by distillation. A vacuum distillation yielded 3.2 g of pure **1c** (10.5 mmol, 14%). B.p. 123–125°C/0.07 mbar. — NMR: See Table 2. — IR:  $\tilde{\nu}$  = 3068 m, 3049 m, 3020 w, 2955 m, 2896 w, 2277 w, 1487 w, 1428 m, 1408 w, 1248 s, 1109 s, 1066 w, 998 w, 837 vs, 803 vs, 783 s, 733 s, 699 vs, 649 m, 475 s. — MS (70 eV), *m/z* (%): 302 (10) [M<sup>+</sup>], 286 (4) [M<sup>+</sup> – CH<sub>3</sub>], 271 (19) [M<sup>+</sup> – 2 Me – H], 135 (100) [SiMe<sub>2</sub>Ph<sup>+</sup>]. — C<sub>16</sub>H<sub>23</sub>PSi<sub>2</sub> (302.5): calcd. C 63.53, H 7.66; found C 63.13, H 7.27.

**Dimeric Bis(tetrahydrofuran)barium Bis[bis(isopropyl)dimethylsilyl]phosphanide] (3B):** A solution of 2.64 g of bis(tetrahydrofuran)barium bis[bis(trimethylsilyl)amide] (4.39 mmol) in 30 ml of tetrahydrofuran was cooled to 0°C. 2.3 ml of phosphane **1b** was added slowly to this solution. After stirring at room temp. for several hours the solvent was distilled off. Then a minimum amount of toluene was added to dissolve the solid at 60°C. On cooling to room temp., 2.84 g of colorless cuboid crystals of **3B** (1.9 mmol, 86%) precipitated from this toluene solution. Decomposition above 90°C. — <sup>1</sup>H NMR ([D<sub>8</sub>]toluene, +50°C):  $\delta$  = 0.35 [d, <sup>3</sup>J(P-H) = 1.2 Hz, SiMe<sub>2</sub>], 1.16 (s, CHMe<sub>2</sub>), 1.46 (m, thf), 1.19 (s, CHMe<sub>2</sub>), 3.73 (m, thf). — <sup>13</sup>C{<sup>1</sup>H} NMR ([D<sub>8</sub>]toluene, +50°C):  $\delta$  = 3.30 [d, <sup>2</sup>J(P-C) = 9.3 Hz, SiMe<sub>2</sub>], 19.23 (s, CHMe<sub>2</sub>), 19.40 (s, CHMe<sub>2</sub>), 25.41 (s, thf), 69.16 (s, thf). — <sup>29</sup>Si{<sup>1</sup>H} NMR ([D<sub>8</sub>]toluene, +50°C):  $\delta$  = 9.03 [d, <sup>1</sup>J(P-Si) = 39.1 Hz]. — <sup>31</sup>P{<sup>1</sup>H} NMR ([D<sub>8</sub>]toluene, +50°C):  $\delta$  = –223 (s, broad). — IR (nujol):  $\tilde{\nu}$  = 1358 m, 1344 w, 1312 w, 1294 w, 1237 vs, 1174 w, 1069 m, 1031 s, 994 s, 965 w, 919 m, 880 s, 810 vs, 750 s, 667 s, 590 s, 476 s, 454 s, 415 m, 327 w, 307 w. — C<sub>56</sub>H<sub>136</sub>Ba<sub>2</sub>O<sub>4</sub>P<sub>4</sub>Si<sub>8</sub> (1496.85): calcd. C 44.93, H 9.16; found C 44.51, H 9.11. — At –60°C monomeric **3A** can be assigned (see text). — <sup>29</sup>Si{<sup>1</sup>H} NMR ([D<sub>8</sub>]toluene):  $\delta$  = 9.43 [d, <sup>1</sup>J(P-Si) = 22.6 Hz]. — <sup>31</sup>P{<sup>1</sup>H} NMR ([D<sub>8</sub>]toluene):  $\delta$  = –274.33.

— Similar results have been obtained from a [D<sub>8</sub>]tetrahydrofuran solution.

**X-ray Structure Determinations**<sup>[18]</sup>: The single crystals covered with nujol were mounted in thinwalled glass capillaries on an automated four-cycle diffractometer (Table 3) by using graphite-monochromated Mo-K $\alpha$  radiation. The unit cells of **2c**, **3A** and **3B** were determined and refined at –80°C from 52, 55, and 32 randomly selected reflections, respectively. The cell parameters are listed in Table 3. — For the solution of the X-ray analytical structures the program packages SHELXTL Plus<sup>[20]</sup> was used. The full-matrix least-squares refinement was carried out with the program SHELXL-93<sup>[21]</sup>. The scattering factors of the neutral atoms<sup>[22]</sup> were used. All nonhydrogen atoms were refined anisotropically. For **2c** all hydrogen atoms were refined isotropically. The silyl substituents at the phosphorus atom P2 of **3A** show a disorder such that there exist two positions of the silicon atoms as well as the CH groups of the isopropyl ligands. The population ratio is 0.6:0.4. The hydrogen atoms were calculated in ideal positions. The hydrogen atoms of the bridging phosphanide ligand of **3B** were refined isotropically. The terminal phosphanide substituent shows a similar disorder as **3A**; however, the population ratio is 0.75:0.25. The hydrogen atoms of this ligand were calculated and added in ideal positions. The H atoms of the tetrahydrofuran molecules were refined isotropically.

Table 3. Crystallographic data of **2c**, **3A**, and **3B** as well as details of the structure solution and refinement procedures

| Compound                                                     | <b>2c</b>                                        | <b>3A</b>                                                                       | <b>3B</b>                                                                       |
|--------------------------------------------------------------|--------------------------------------------------|---------------------------------------------------------------------------------|---------------------------------------------------------------------------------|
| Empirical formula                                            | PSi <sub>3</sub> C <sub>24</sub> H <sub>33</sub> | BaP <sub>2</sub> Si <sub>4</sub> O <sub>4</sub> C <sub>36</sub> H <sub>84</sub> | BaP <sub>2</sub> Si <sub>4</sub> O <sub>2</sub> C <sub>28</sub> H <sub>68</sub> |
| Molecular mass (g mol <sup>–1</sup> )                        | 436.74                                           | 892.67                                                                          | 748.46                                                                          |
| <i>T</i> (°C)                                                | –80                                              | –80                                                                             | –80                                                                             |
| Space group <sup>[19]</sup>                                  | <i>P</i> $\bar{3}$ (No. 147)                     | <i>P</i> 2 <sub>1</sub> /c (No. 14)                                             | <i>P</i> $\bar{1}$ (No. 2)                                                      |
| Unit cell dimensions                                         |                                                  |                                                                                 |                                                                                 |
| <i>a</i> (pm)                                                | 1552.1(2)                                        | 2039.7(6)                                                                       | 1138.3(2)                                                                       |
| <i>b</i> (pm)                                                | 1552.1(2)                                        | 1294.2(3)                                                                       | 1294.2(3)                                                                       |
| <i>c</i> (pm)                                                | 656.5(1)                                         | 1924.3(3)                                                                       | 1614.4(3)                                                                       |
| $\alpha$ (°)                                                 | 90                                               | 90                                                                              | 69.57(3)                                                                        |
| $\beta$ (°)                                                  | 90                                               | 98.94(2)                                                                        | 76.94(3)                                                                        |
| $\gamma$ (°)                                                 | 120                                              | 90                                                                              | 67.54(3)                                                                        |
| <i>V</i> (nm <sup>3</sup> )                                  | 1.3696(3)                                        | 5.018(2)                                                                        | 2.0443(7)                                                                       |
| <i>Z</i>                                                     | 2                                                | 4                                                                               | 2 (1 dimer)                                                                     |
| <i>D</i> <sub>calcd</sub> (g cm <sup>–3</sup> )              | 1.059                                            | 1.182                                                                           | 1.216                                                                           |
| <i>f</i> (pm)                                                | 71.073                                           | 71.073                                                                          | 71.073                                                                          |
| $\mu$ (mm <sup>–1</sup> )                                    | 0.239                                            | 0.981                                                                           | 1.188                                                                           |
| <i>F</i> (000)                                               | 468                                              | 1896                                                                            | 788                                                                             |
| Diffractometer                                               | Siemens P4                                       | Siemens P4                                                                      | Syntex P2 <sub>1</sub>                                                          |
| Scan mode, width (°)                                         | $\omega$ scan, 1.5                               | $\omega$ scan, 1.2                                                              | Wyckoff, 1.2                                                                    |
| Scan range (°)                                               | 3.2 < 2 $\theta$ < 56                            | 3.7 < 2 $\theta$ < 50.4                                                         | 3.5 < 2 $\theta$ < 52                                                           |
| Measured data                                                | 4600                                             | 9207                                                                            | 8029                                                                            |
| Unique data ( <i>R</i> <sub>int</sub> )                      | 2203 (0.0433)                                    | 8929 (0.0260)                                                                   | 8011 (0.0288)                                                                   |
| No. of parameters                                            | 130                                              | 421                                                                             | 532                                                                             |
| Goodness-of-fit <i>s</i> on <i>F</i> <sup>2</sup> [a]        | 1.116                                            | 1.363                                                                           | 1.066                                                                           |
| <i>R</i> indices [all data]                                  |                                                  |                                                                                 |                                                                                 |
| <i>R</i> <sub>1</sub> [b]                                    | 0.0561                                           | 0.0723                                                                          | 0.0662                                                                          |
| <i>wR</i> <sub>2</sub> [b]                                   | 0.1227                                           | 0.1328                                                                          | 0.1235                                                                          |
| <i>R</i> indices [ <i>I</i> > 2 $\sigma$ ( <i>I</i> ), data] | 2060                                             | 6942                                                                            | 6579                                                                            |
| <i>R</i> <sub>1</sub> [b]                                    | 0.0453                                           | 0.0501                                                                          | 0.0488                                                                          |
| <i>wR</i> <sub>2</sub> [b]                                   | 0.1187                                           | 0.1210                                                                          | 0.1122                                                                          |
| Residual density (e nm <sup>–3</sup> )                       | 856 to –239                                      | 971 to –490                                                                     | 1190 to –1548                                                                   |

[a]  $s = \{\sum [w(F_o^2 - F_c^2)^2] / (N_o - N_c)\}^{1/2}$ . — [b] Definition of the *R* indices:  $R_1 = (\sum \|F_o - F_c\|) / \sum F_o$ ;  $wR_2 = \{\sum [w(F_o^2 - F_c^2)^2] / \sum w(F_o^2)\}^{1/2}$  with  $w^{-1} = \sigma^2(F_o^2) + (aP)^2$ .

[1] M. Westerhausen, W. Schwarz, *Z. Anorg. Allg. Chem.* **1992**, 609, 39; M. Westerhausen, W. Schwarz, *ibid.* **1991**, 604, 127; M. Westerhausen, W. Schwarz, *ibid.* **1991**, 606, 177; B. A. Vaartstra, J. C. Huffman, W. E. Streib, K. G. Caulton, *Inorg. Chem.* **1991**, 30, 121.

[2] M. Westerhausen, *Inorg. Chem.* **1991**, 30, 96.

[3] M. Westerhausen, *J. Organomet. Chem.* **1994**, 479, 141.

- [4] G. W. Rabe, J. Riede, A. Schier, *Organometallics* **1996**, *15*, 439.
- [5] Review: F. Pauer, P. P. Power in *Lithium Chemistry: a Theoretical and Experimental Overview* (Eds.: A.-M. Sapse, P. v. R. Schleyer), Wiley-Interscience, New York, **1995**, chapter 9; see also: E. Hey-Hawkins, E. Sattler, *J. Chem. Soc., Chem. Commun.* **1992**, 775; G. Becker, H. M. Hartmann, W. Schwarz, *Z. Anorg. Allg. Chem.* **1989**, 577, 9; E. Hey, P. B. Hitchcock, M. F. Lappert, A. K. Rai, *J. Organomet. Chem.* **1987**, 325, 1.
- [6] S. C. Goel, M. Y. Chiang, W. E. Buhro, *J. Am. Chem. Soc.* **1990**, *112*, 5636; S. C. Goel, M. Y. Chiang, D. J. Rauscher, W. E. Buhro, *ibid.* **1993**, *115*, 160; B. Rademacher, W. Schwarz, M. Westerhausen, *Z. Anorg. Allg. Chem.* **1995**, 621, 287.
- [7] M. Westerhausen, M. Hartmann, W. Schwarz, *Inorg. Chem.* **1996**, 35, 2421.
- [8] M. Westerhausen, R. Löw, Universität Stuttgart, unpublished results; for the magnesium and calcium bis(phosphanides) see also: M. Westerhausen, R. Löw, W. Schwarz, *J. Organomet. Chem.* **1996**, 513, 213.
- [9] H. Bürger, U. Goetze, *J. Organomet. Chem.* **1968**, *12*, 451; E. Fluck, H. Bürger, U. Goetze, *Z. Naturforsch., Part B*, **1967**, *22*, 912; W. Uhlig, A. Tzschach, *Z. Anorg. Allg. Chem.* **1989**, 576, 281.
- [10] G. Becker, H. Schmidt, G. Uhl, W. Uhl, *Inorg. Synth.* **1990**, 27, 243.
- [11] H. Schäfer, G. Fritz, W. Hölderich, *Z. Anorg. Allg. Chem.* **1977**, 428, 222; M. Baudler, K. Glinka, *Inorg. Synth.* **1990**, 27, 228.
- [12] K. Hassler, *Monatsh. Chem.* **1988**, *119*, 851; **1988**, *119*, 863.
- [13] G. A. Forsyth, D. W. H. Rankin, H. E. Robertson, *J. Mol. Struct.* **1990**, 239, 209.
- [14] M. Westerhausen, A. Pfitzner, *J. Organomet. Chem.* **1995**, 487, 187.
- [15] M. Westerhausen, W. Schwarz, *J. Organomet. Chem.* **1993**, 463, 51.
- [16] M. Westerhausen, H.-D. Hausen, W. Schwarz, *Z. Anorg. Allg. Chem.* **1995**, 621, 877.
- [17] M. Schütze, *Angew. Chem.* **1958**, *70*, 697.
- [18] Further details of the crystal structure investigations are available on request from the Fachinformationszentrum Karlsruhe, D-76344 Eggenstein-Leopoldshafen, on quoting the depository numbers CSD-405066, -405067, and -405065 for **2c**, **3A**, and **3B**, respectively.
- [19] T. Hahn (Ed.), *International Tables for Crystallography*, vol. A, *Space Group Symmetry*, 2nd Ed., D. Reidel, Dordrecht, **1984**.
- [20] SHELXLTL Plus, Siemens Analytical X-Ray Instruments, Inc., **1980**.
- [21] G. M. Sheldrick, SHELXL-93, Universität Göttingen, **1993**.
- [22] D. T. Comer, J. B. Mann, *Acta Crystallogr., Sect. A*, **1968**, *24*, 321; R. F. Stewart, E. R. Davidson, W. T. Simpson, *J. Chem. Phys.* **1965**, *42*, 3175.

[96071]